Snow Water Equivalent Prediction for Northern New Mexico Using the Convolutional LSTM Machine Learning Method

Student Researcher: Ujjwal Marasini
Faculty Advisor: Dr. Huidae Cho
Department of Civil and Environmental Engineering

A Final report submitted to New Mexico Water Resources Research Institute

Major: Civil Engineering
Concentration: Water Resources Engineering

NEW MEXICO STATE UNIVERSITY
LAS CRUCES, NEW MEXICO

September, 2025

Contents

1 Introduction

1.1 Problem Statement

In New Mexico, earlier snow melting is anticipated because global climate-driven models projected an average temperature increase across the state between 5°F and 7°F over the next 50 years (Dunbar et al., 2022). It will lead to the lack of water during the Summer and can even cause snowmelt flooding. For example, Harpold et al. (2014) suggested an increment in the snow sublimation in the area with a high atmospheric water demand. Further, the northern tier states and mountainous areas of the U.S. are particularly susceptible to snowmelt flooding (National Weather Service, 2024). However, based on an extensive literature review, there are no studies focusing on the long-term forecasting of Snow Water Equivalent (SWE) in northern New Mexico. This study aims to fill this gap by making a long-term forecast of SWE for the upper part of the state. Cui et al. (2022) explored the ability of the Long Short-Term Memory (LSTM) machine learning method in forecasting SWE in California and Nevada. Similarly, Song et al. (2024) integrated the 30-day-lagged SWE into LSTM in the western United States to improve future prediction.

1.2 Importance of SWE Prediction

Snow pack is the part of hydrological cycle and Snow water equivalent (SWE) determines the amount of water available in the snowpack. Measuring the amount of water in snow is challenging because the water content in each depth of snow varies depending on air temperature. Accurately predicting SWE is essential for efficient water resource management, particularly in areas where snowmelt is the main source of freshwater. This information also provides valuable information for estimating seasonal water availability. Various storms produce different types of snow with varying water content. Warmer storms can result in two inches of sleet from an inch of rain, while colder storms may produce over 50 inches of light, powdery snow from the same amount of rainfall. Throughout the winter, the diversity of storm conditions means that snow depth alone is not a reliable indicator of water content. Due to this variability, measuring SWE provides a more accurate assessment of the actual water stored within the snowpack.

Reliable SWE predictions are crucial for forecasting streamflow, managing reservoirs, and maintaining a sustainable water supply for agricultural, municipal, and ecological purposes. This is especially important in semi-arid and arid regions like the Northern part of the United States, where snowmelt plays a significant role in replenishing river systems and groundwater resources. In this region, snowpack is one of the most important resources economically and ecologically. In the West, mountains act as natural reservoirs by collecting snow in the winter and releasing it in the spring as temperatures increase. Between 60 and 70% of water supplies come from snowmelt, with high mountain regions being on the high end of that range.

In New Mexico, seasonal snowfall varies due to its unique and extensive topography (National Weather Service, 2025). The elevation varies from 3,000 ft (Southeast Plains) to 13, 000 ft (Wheeler Peak), with higher elevations typically accumulating more snow and experiencing snowfall earlier and later in the season than lower areas. In Northern New Mexico, snowpack is essential because the water from the snow melting is used for drinking water, irrigation systems, industrial applications, and water supply. In this region, the snowpack conditions are showing extreme differences between 2025 and 2024, presenting a grim outlook for the state's forecast basins. This suggests that hydrologists anticipate significantly reduced water availability in river basins due to below-average snowpack levels. For instance, as of February 1, 2025, New Mexico's snowpack was just over 55% of the median for that date, with some basins recording even lower levels. Such shortfalls pose substantial challenges for water resource management, agriculture, and ecological systems that depend on consistent water supplies.

1.3 Objectives of the Project

The proposed project will evaluate the ability of the Convolutional LSTM (ConvLSTM) model in predicting SWE in the study area. The specific objectives of the study are: The specific objectives of the study are:

1. To create a ConvLSTM machine learning model for SWE in northern New Mexico.
2. To perform the sensitivity analysis on input parameters.
3. To forecast changes in SWE for the next 30 years under different climate change scenarios using CMIP6 data.

2 Background and Literature Review

2.1 Summary of SWE Modeling Techniques

2.1.1 Field Measurements

This method is regarded as the most direct and reliable way to measure SWE because it involves physically sampling or monitoring the snowpack using specialized equipment. The field measurements provide tangible, on-the-ground data that reflect actual snowpack conditions at a specific location and time. Field measurement data are also used for calibrating and validating the accuracy of models, remote sensing estimates, and developing empirical relationships between observed SWE and estimated SWE.

1. **Snow Sampler**
   Snow Sampler (also known as Federal snow sampler) is a device that measures the SWE directly. This device consists of an aluminum snow tube and a spring scale with calibrated markings and a cutting edge at the bottom. To measure the snow depth snow tube is pushed vertically through the snowpack to the ground surface, and a core is extracted. In this process, 5 to 10 measurements are taken at regular intervals along the snow course. To obtain an accurate snow core sample, the tube reaches the ground, which can be ensured by checking the base of the tube for soil. Once soil is confirmed and cleared from the tube, the Snow Water Equivalent (SWE) is measured by weighing the tube with the collected snow core and then subtracting the weight of the empty tube. The process is typically repeated across multiple points along a snow course, and the average of all samples is calculated to represent the total SWE for that area.

2. **Snow Pillows**
   A snow pillow, developed in the early 1960s, is a device to measure snowpack for automatic measurements of SWE. It consists of large, flat, flexible bladders filled with anti-freeze or glycol solution, installed on the ground and connected to pressure sensors. The snow pillow measures the water equivalent of the snowpack based on the hydrostatic pressure created by overlying snow. Any discrepancy due to bridging is minimized by the large dimension of the pillow, typically 9 square meters. These systems provide continuous, real-time data and are commonly deployed at SNOTEL sites across the western U.S., including New Mexico.

3. **Gamma Radiation Attenuation**
   Incoming, background cosmic radiation constantly fluxes through the earth's atmosphere. The high-energy gamma portion of this radiation penetrates many terrestrial objects, including the winter snowpack. The attenuation of this radiation is exponentially related to the mass of the medium through which it penetrates. This gamma sensor, measuring energy levels between 5 and 15MeV, has proved to be an accurate, reliable, non-invasive, non-mechanical instrument to measure the total snow water equivalent of a snowpack (Osterhuber et al. 1998).

4. **Snow Density Profiling**
   Snow Density Profiling is a manual technique used to estimate Snow Water Equivalent (SWE) by measuring the density of snow at different depths within the snowpack. This method involves extracting samples of known volume from various snow layers using tools such as snow cutters or density kits. The mass of each sample is measured, and density is calculated by dividing the mass by volume. SWE is then determined by integrating these density measurements across the entire snow depth. This technique provides detailed profiles of snow density, essential for understanding snow accumulation, melt processes, and overall water content. However, it is labor-intensive and limited to specific sites, making it impractical for large-scale or continuous monitoring (Sturm et al., 2010).

5. **Ground-Penetrating Radar (GPR)**
   Ground-penetrating radar (GPR) is an effective tool for measuring snow water equivalent (SWE) because of the close relationship between snow density and radar velocity. However, the standard methods of measuring radar speed can be time-consuming (Clair and Holbrook, 2017).

2.1.2 Empirical and Statistical Methods

The empirical models include static and dynamic algorithms, which are established via the bright temperature differences at different frequencies. The static algorithms calculate SWE (or snow depth) using a linear regression between snow water equivalent and brightness temperature gradient for a snowpack with temporally and spatially constant properties, as SWE = A+B× TB

where SWE is the snow water equivalent (mm), TB is the vertically (or horizontally) polarized brightness temperature difference between low (18 or 19 GHz) and high (37 or 85 GHz) frequency, and A and B are the offset (mm) and slope (mm/K), respectively. The coefficients A and B are obtained by fitting with experimental data. The NASA algorithm is the simplest example of a SWE static algorithm, which is derived from the SMMR sensor: SWE = 4.8 × (TB,18H -TB,37H)

where TB,18H and TB,37H indicate the horizontally polarized brightness temperatures (K) at 18 and 37 GHz, respectively. TB is calculated using RTE for a homogeneous snowpack with a constant snow grain size of 0.3 mm and a constant density of 300 kg/m3. The NASA algorithm can be used only for SWE less than 300 mm because the brightness temperature difference for greater SWE becomes saturated. In addition, the model is not suitable for various snow grain sizes except 0.3 mm. SWE estimation is greatly complicated when the surface is covered with vegetation, as the canopy coverage affects the microwave emitted from the snowpack. To consider the forest effect, the NASA 96 algorithm, which is the extended version of the NASA model, was developed to provide global SWE inversion.

2.1.3 Physically Based Models

Physically based models simulate Snow Water Equivalent (SWE) by accounting for the fundamental processes governing snowpack accumulation, compaction, metamorphism, and melt. These models use detailed meteorological inputs, such as temperature, precipitation, wind speed, humidity, and radiation, to simulate the energy and mass balance of snowpacks. Unlike statistical or empirical models, physically based models aim to capture the actual physical processes that affect snow dynamics, making them more robust and applicable across various conditions and climates. Some commonly used physically based models for SWE include:

1. **SNOWPACK Model**
   This model is developed by the Swiss Federal Institute for Snow and Avalanche Research (SLF), SNOWPACK simulates the evolution of snow layers based on heat and mass transfer, including meltwater percolation and refreezing processes. It is commonly used for avalanche forecasting and hydrological research (Bartelt & Lehning, 2002).

2. **Noah-MP (Noah-Multiparameterization) Model**
   Noah-MP simulates snowpack processes, including sublimation, compaction, and melt, with multiple parameterization options for vegetation, soil, and hydrology (Niu et al., 2011). An improved land surface model has been integrated into the Weather Research and Forecasting (WRF) model to enhance its simulation of land-atmosphere interactions and provide more accurate weather forecasts.

3. **VIC (Variable Infiltration Capacity) Model**
   VIC is a macro scale hydrological model that corporates snow accumulation and melt processes bacekd on energy balance principles. This model has been widely used in streaflow forecasting and climate change studies (Liang et al., 1994).

4. **CLM (Community Land Model**
   CLM model simulates energy and water fluxes across the land surface, including snow dynamics. It is part of the CESM (Community Earth System Model) and is used for climate and hydrological research (Lawrence et al., 2011). Physically based models offer a detailed, process-oriented approach to simulating SWE, providing accurate results when properly calibrated and validated. They are particularly valuable for understanding the interactions between snowpack and other components of the hydrological cycle. However, these models require extensive meteorological input data and computational resources, making them challenging to apply over large areas or in data-scarce regions.

2.1.4 Remote Sensing Methods

Remote sensing methods are used to estimate SWE over large areas, where field measurements are inaccessible. They rely on satellite, and ground-based sensors to gather on snow depth, extent, density and related properties. Numbers of methods are used to estimate SWE by remote sensing methods. Passive microwave sensors (Chang et al., 1987; Kelly et al., 2003), Synthetic Aperture Radar (SAR) (Rott et al., 2010; Lievens et al., 2019), Lidar systems (Painter et al., 2016), optical and multispectral imaging tools (Hall et al., 2002; Dozier, 1989), Data fusion and assimilation techniques (Margulis et al., 2015) are commonly used techniques used in remote sensing. This method offers broad spatial coverage but may be affected by factors such as terrain, vegetation, and snow conditions, necessitating validation with in-situ measurements.

2.1.5 Machine Learning Methods

Machine learning techniques are increasingly applied to estimate Snow Water Equivalent (SWE) by learning patterns from large datasets of meteorological inputs, snow observations, and remote sensing data. Unlike traditional models, machine learning models can capture complex, nonlinear relationships and improve predictive accuracy through training. Common approaches include Artificial Neural Networks (ANN), Random Forests, Support Vector Machines (SVM), Convolutional Neural Networks (CNN), and Convolutional LSTM (ConvLSTM). ConvLSTM is particularly suitable for SWE prediction because it combines spatial and temporal features, making it effective at handling time-series data with spatial dependencies. These methods excel in scenarios where large datasets are available for training, but their performance heavily depends on data quality, training process, and the ability to generalize to new conditions. While machine learning models can provide high accuracy, they often require significant computational resources and extensive tuning for optimal performance.

2.2 Justification for Using ConvLSTM

ConvLSTM model covers both spatial and temporal dependencies in comlex evironmental systems so, this method is suitable for predicting SWE. ConvLSTM model combines the LSTM modeling temporal sequences and Convo-

lutional Neural Networks (CNNs) for extracting spatial features. So, this is ideal to analyses the time-series data satellite imagery (Shi et al., 2015).

Traditional machine learning models, such as ANN and SVM, are limited in their ability to model spatially distributed data and temporal dependencies simultaneously. While CNNs can effectively capture spatial patterns, they lack the capacity to model sequential dependencies over time. Conversely, LSTM networks excel at handling temporal relationships but are not optimized for spatial feature extraction. ConvLSTM addresses these limitations by introducing convolutional operations within the LSTM architecture, allowing it to process spatiotemporal data more efficiently and accurately (Shi et al., 2015; Wang et al., 2020).

ConvLSTM is particularly useful for SWE prediction as snowpack dynamics are influenced by both spatial heterogeneity (e.g., topography, vegetation, land cover) and temporal variability (e.g., seasonal changes, precipitation events). By applying convolutional filters within the recurrent LSTM cells, ConvLSTM can capture localized spatial features while simultaneously learning temporal dependencies, resulting in improved predictive performance over traditional models (Xingjian et al., 2015; Bi et al., 2020). This advantage is especially significant for SWE prediction in mountainous and heterogeneous landscapes like Northern New Mexico, where the spatial distribution of snowpack is highly variable.

Furthermore, ConvLSTM has demonstrated superior performance in various hydrological and environmental prediction tasks, such as precipitation nowcasting, streamflow prediction, and snow depth estimation (Shi et al., 2015; Bi et al., 2020; Wang et al., 2020). Its ability to effectively handle gridded inputs and produce high-resolution outputs makes it a powerful tool for SWE prediction using meteorological and remote sensing data. Additionally, ConvLSTM offers improved generalization capabilities compared to simpler models when trained on diverse datasets, making it a promising approach for large-scale, data-driven SWE prediction efforts.

3 Materials and Methods

3.1 Study Area

The study area (Figure 1) is located in the southwest United States. It extends from 103°W to 109°W and 32°N to 37°N. This region is characterized by diverse topography, including the southern Rocky Mountains, vast plateaus, deserts like the Chihuahuan Desert, and deep canyons, the northern and western regions dominated by mountainous areas such as the Sangre de Cristo and San Juan ranges, while the southern part is predominantly arid. Hydrologically, New Mexico is drained by several river systems, including the Rio Grande.

New Mexico has a varied climate, with cooler temperatures in the mountains and hot, dry summers with mild winters in the desert. The state gets monsoonal rains in summer and snow in the mountains during winter, creating a mixture of desert, steppe, and alpine climates depending on elevation. This results in a diverse environment with different seasonal changes throughout the state. Snowfall is influenced by mountain barriers and winter storms from the Pacific, which bring snow to the higher elevations and central parts of the state. This region experiences heavy snowfall in its northern and higher elevations, such as the Sangre de Cristo and San Juan Mountains, while the southern arid regions, such as the Chihuahuan Desert, see much lighter snow.

3.2 Necessary Datasets and their Sources

1. **Precipitation and Temperature Datasets**
   The long term annual average precipitation and temperature datasets are obtained from PRISM datasets. These datasets are spatial climate data, primarily for the United States, which provide estimates of seven primary climate elements. These long-term data sets are modeled with PRISM using a Digital Elevation Model (DEM) as a predictor grid. These datasets are downloaded using the call function from Python's subprocess module. This function executes the wget command, which downloads files raining Deep Neural

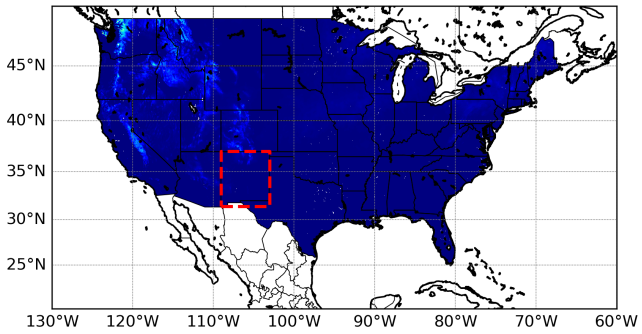

Figure 1: Study Area

Networks is complicated by the fact that the distribution of each layer's inputs changes during training, as the parameters of the previous layers change. This slows down the training by requiring lower learning rates and careful parameter initialization, and makes it notoriously hard to train models with saturating nonlinearities. We refer to this phenomenon as internal covariate shift, and address the problem by normalizing layer inputs. Our method draws its strength from making normalization a part of the model architecture and performing the normalization for each training mini-batch. Batch Normalization allows us to use much higher learning rates and be less careful about initialization. It also acts as a regularizer, in some cases eliminating the need for Dropout. Applied to a state-of-the-art image classification model, Batch Normalization achieves the same accuracy with 14 times fewer training steps, and beats the original model by a significant margin. Using an ensemble of batch-normalized networks, we improve upon the best published result on ImageNet classification: reaching 4.9 % top-5 validation error (and 4.8 % test error), exceeding the accuracy of human raters.

2. **Snow Water Equivalent Datasets**
   The snow water equivalent datasets are obtained form National Snow and Ice Data Center. These data sets are stored as the NetCDF (Network Common Data Form), a file format for storing multidimensional scientific data. These datasets are downloaded using the similar procedure as precipitation and temperature datasets. The Figure 2 represents the snow depth measurement stations in the New Mexico and the Figure 3 is the sample day of one particular day. The dataset represents Snow Water Equivalent (SWE) data with a three-dimensional array of shape (365, 621, 1405). The three dimensions correspond to time, latitude, and longitude. The time dimension has 365 data points, which correspond to daily measurements. The latitude dimension contains 621 points, while the longitude dimension holds 1405 points, reflecting the geographic coverage of the data. This dataset captures the variation of SWE across a specific geographic region and over a full year, providing insights into the amount of water stored in the snowpack throughout that period. Each grid in this datasets represents 2.5' and based on this latitude (103°W to 109°W) and longitude (32°N to 37°N) of New Mexico, grid 168 to 290 represents the latitude and 876 to 1021 represents the longitude of study area.

3.3 Data Pre-processing

3.3.1 Epoch and batch size

The number of epochs and batch size are crucial hyperparameters that significantly impact model training, speed, and quality. An epoch is a complete pass of the entire dataset through the model during training, determining how many times the model adjusts its weights based on the data. Too few epochs can lead to underfitting, where the model fails to learn important patterns, while too many can cause overfitting, where the model learns

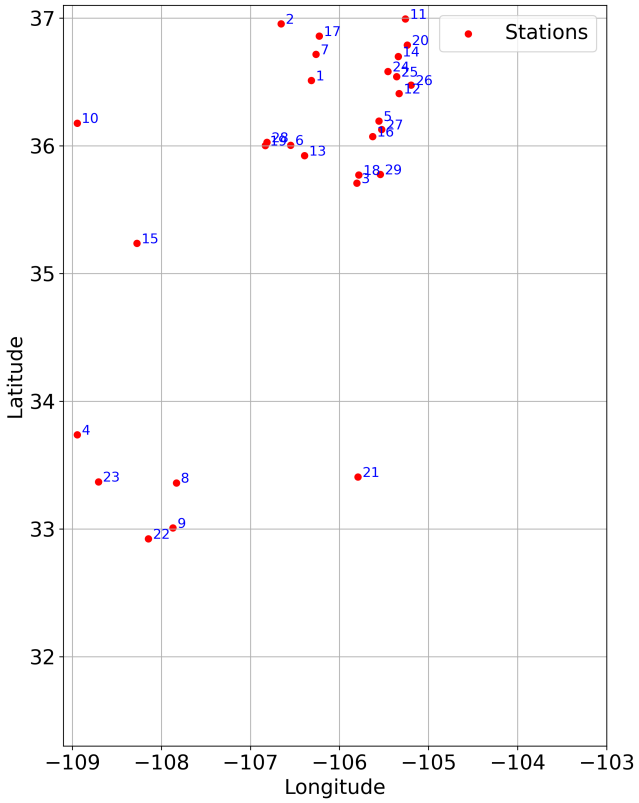

Figure 2: Snow measurement stations in New Mexico

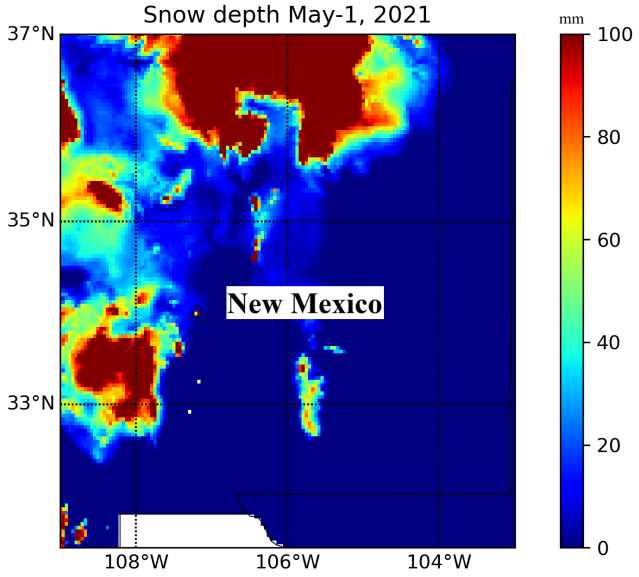

Figure 3: Snow depth of New Mexico, measured on May 1, 2021

noise and irrelevant details. To avoid overfitting, techniques like EarlyStopping can be applied to halt training when validation performance starts to deteriorate. The ideal number of epochs is achieved by balancing model performance on training and validation sets.

Batch size refers to the number of training samples processed before the model's weights are updated. Smaller batch sizes provide more frequent updates but may result in noisy gradient estimates, leading to unstable training. Larger batch sizes offer more stable gradients and efficient use of hardware but can cause the model to get stuck in local minima. The choice of batch size depends on available computational resources, dataset size, and optimizer type. While mini-batch gradient descent offers a balanced approach between stability and frequency of updates, adaptive optimizers like Adam or RMSProp often perform well with moderate batch sizes (32-64). Finding the right combination of epochs and batch size requires experimentation and monitoring of validation performance.

3.4 Batch Normalization Layer

Batch normalization applies a transformation that maintains the mean output close to 0 and the output standard deviation close to 1. This works differently during training and during inference. Training Deep Neural Networks is complicated by the fact that the distribution of each layer's input changes during training, as the parameters of the previous layers change. This slows down the training by requiring lower learning rates and careful parameter initialization, and makes it notoriously hard to train models with saturating nonlinearities.

Training Deep Neural Networks is complicated by the fact that the distribution of each layer's inputs changes during training, as the parameters of the previous layers change. This slows down the training by requiring lower learning rates and careful parameter initialization, and makes it notoriously hard to train models with saturating nonlinearities. We refer to this phenomenon as internal covariate shift, and address the problem by normalizing layer inputs. Our method draws its strength from making normalization a part of the model architecture and performing the normalization for each training mini-batch. Batch Normalization allows us to use much higher learning rates and be less careful about initialization. It also acts as a regularizer, in some cases eliminating the need for Dropout. Applied to a state-of-the-art image classification model, Batch Normalization achieves the same accuracy with 14 times fewer training steps, and beats the original model by a significant margin. Using an ensemble of batch-normalized networks, we improve upon the best published result on ImageNet classification: reaching 4.9 % top-5 validation error (and 4.8 % test error), exceeding the accuracy of human raters.

During training the layer normalizes its outputs using the mean and standard deviation of the current batch of inputs. In keras and Tensorflow the training arguments are automatically handled during the training phase, so this is not necessary to mention. During testing the layer normalizes its output using a moving average of the mean and standard deviation of the batches it has seen during training.

3.5 ConvLSTM model Development

The development of the ConvLSTM model for predicting Snow Water Equivalent (SWE) involves several key steps, including defining the model architecture, preparing input data, training the model, evaluating performance, and optimizing hyperparameters. ConvLSTM is chosen for its ability to capture both spatial and temporal dependencies, making it ideal for handling complex datasets like snowpack dynamics influenced by topography, meteorology, and seasonal changes.

The original version of the code was developed by Dr. Baokun Li at the Computational Lab for Advanced Water Resources Informatics and Modeling (CLAWRIM), with a focus on hydrologic modeling in the western United States. His work provided a strong foundation for data processing, model setup, and simulation workflows. For the purpose of this study, I revised and adapted the code to suit the specific characteristics and requirements of the selected study area. This included modifications to input data handling, spatial configurations, and model parameters to ensure compatibility with local conditions and datasets.

3.5.1 Model Architecture

The ConvLSTM model architecture integrates convolutional layers and LSTM layers to process spatiotemporal data. Unlike traditional LSTM models, ConvLSTM applies convolution operations within the recurrent cells, allowing it to preserve spatial relationships while learning temporal dependencies. This makes it particularly effective for datasets with gridded inputs such as satellite imagery, meteorological maps, or spatially distributed ground observations (Shi et al., 2015). The architecture consists of:

1. Input Layers
This accepts multi-dimensional data (e.g., precipitation, temperature, swe data) over New Mexico.

2. Convolutional LSTM Layers
This extracts spatial features and learns temporal sequences through convolutional operations integrated within LSTM cells.

3. Pooling Layers (Optional)
This reduces spatial dimensions to enhance computational efficiency.

4. Fully Connected Layers
It produces predictions of SWE based on learned features.

5. Output Layer
This layer generates SWE estimates for the desired spatial and temporal resolution.

3.5.2 Code Explanation

1. ConvLSTM2D Layer (1st Layer)

```
x = layers.ConvLSTM2D(
    filters=64,
    kernel_size=(5, 5),
    padding="same",
    return_sequences=True,
    activation="relu",
)(inp)
```

filters=64: Specifies the number of convolutional filters to be applied. A higher number of filters allows the model to learn more complex spatial features.

kernel_size=(5,5): Defines the size of the convolutional window. A larger kernel size helps capture broader spatial features.

padding = "same": Ensures the output size matches the input size by padding the borders appropriately.

return_sequences = True: Ensures that the full sequence of outputs is returned, allowing the model to process multi-step sequences.

activation = "relu": Applies the ReLU activation function to introduce non-linearity, enhancing the model's ability to learn complex patterns.

2. Batch Normalization (1st Layer)

```
x = layers.BatchNormalization()(x)
```

1. Normalizes the output from the previous ConvLSTM2D layer, ensuring a stable learning process by keeping the activations within a controlled range.

2. Helps prevent overfitting and accelerates model training.

3. ConvLSTM2D Layer (2nd Layer)

```
x = layers.ConvLSTM2D(
    filters=64,
    kernel_size=(3, 3),
    padding="same",
    return_sequences=True,
    activation="relu",
)(inp)
```

1. Similar to the first ConvLSTM2D layer but with a smaller kernel size (3x3).

2. The reduced kernel size focuses on capturing finer spatial details.

4. Batch Normalization (2nd Layer)

```
x = layers.BatchNormalization()(x)
```

1. Normalizes the output from the previous layer to enhance training stability.

5. ConvLSTM2D Layer (3rd Layer)

```
x = layers.ConvLSTM2D(
    filters=64,
    kernel_size=(1, 1),
    padding="same",
    return_sequences=True,
    activation="relu",
)(inp)
```

1. Uses a 1x1 kernel size which acts as a bottleneck layer to reduce the number of parameters and enhance model efficiency.

2. Useful for dimensionality reduction and refining learned features before final output.

6. Conv3D Layer (Output Layer)

```
x = layers.Conv3D(
    filters=1, kernel_size=(3, 3, 3), activation="sigmoid", padding="same"
)(x)
```

filters=1 1. Outputs a single channel prediction, which corresponds to the estimated SWE values.

kernel_size = (3,3,3) 2. Performs 3D convolution to aggregate spatial and temporal features.

activation="sigmoid" 3. Produces normalized outputs between 0 and 1, suitable for generating predictions.

padding="same" 4. Ensures that the output dimensions match the input dimensions.

3.5.3 Implementation Tools

1. Programming Language: Python

2. Libraries:

```
import numpy as np
import pandas as pd
import matplotlib.pyplot as plt
```

```
from tensorflow.keras.models import Sequential
from tensorflow.keras.layers import LSTM, Embedding, Dense, Dropout, Bidirectional
from tensorflow.keras.preprocessing.sequence import pad_sequences
from sklearn.model_selection import train_test_split
```

3. Computational Resources:
For deep learning model training, computational efficiency can be significantly improved using either GPUs (Graphics Processing Units) or HPC (High-Performance Computing) clusters. GPUs are optimized for parallel processing, making them ideal for accelerating tensor operations in deep learning frameworks like TensorFlow and PyTorch. They are cost-effective for small to mid-sized projects, with cloud-based options available for scalability. However, GPUs are limited by memory (e.g., 24GB–80GB VRAM) and may struggle with extremely large datasets. In contrast, HPC clusters offer distributed computing across multiple nodes, providing large memory, high-speed networking (e.g., InfiniBand), and scalability for massive datasets and complex simulations. While HPC is highly efficient for large-scale training, it requires complex setup, job scheduling (e.g., SLURM), and higher costs. Choosing between GPU and HPC depends on project scale, budget, and computational requirements, with GPUs being suitable for individual research and HPC for high-end scientific computing.

4 Results

The primary objective of this study was to develop and evaluate a ConvLSTM machine learning model for Snow Water Equivalent (SWE) prediction in northern New Mexico. The model was trained using spatial and temporal input data and tested over multiple forecast horizons (1–5 days). The performance evaluation demonstrates that the ConvLSTM model achieved high predictive skill across most stations, with efficiency values ranging between 0.85 and 0.99 (Table 1). The spatial prediction maps (Fig. 9) further confirm that the model effectively reproduced SWE distribution across the region, capturing both accumulation and melt dynamics. While the 1-day and 2-day forecasts showed the highest accuracy, the model retained strong predictive performance even at 5-day forecasts, with only minor degradation observed at a few stations. These results highlight the ConvLSTM model's ability to reliably capture both temporal trends and spatial variability of SWE, thereby fulfilling the study's primary objective.

The ConvLSTM model developed for predicting Snow Water Equivalent (SWE) in New Mexico demonstrated strong performance in capturing the dynamics of snow accumulation and melting throughout the study period. In some station COnvLSTM performed better than the LSTM model and some statistical techniques based on the RMSE value. The model yielded higher efficiency in regions with coarser snow measurement data. Overall, the results validate the use of deep learning models with spatiotemporal awareness like ConvLSTM for improving SWE prediction in snow-dominated watersheds.

4.1 Statistical Analysis

To evaluate the performance of model in predicting Nash Suctcliffe efficiency value was employed. The model achieved higher efficiency in most of the location and in some cases it is low. Table 1 summarizes the efficiency in 29 stations in New Mexico. This Table-1 and Figure 4(a) presents the geographic coordinate of monitoring stations along with the efficiency in the corresponding stations as shown in Figure 4(b). The relative performance of ConvLSTM model in different station approximately ranges from approximately 0.37 to 0.94.

4.1.1 Prediction Using 1-Day Data

The Snow Water Equivalent (SWE) analysis for New Mexico using one-day prediction data is presented in Figure 4. Panel (a) shows the model efficiency across different stations, where most stations achieve high values (close to

0.9–1.0), indicating strong predictive skill, while a few outliers exhibit much lower efficiencies, suggesting localized challenges likely due to site-specific variability or data limitations. Panel (b) compares observed versus predicted SWE time series, demonstrating that the model captures the seasonal accumulation and melt cycles with close alignment of peaks and trends, although minor deviations remain during high-accumulation periods. Together, these results suggest that the model is capable of reproducing regional SWE dynamics with daily input data, but further refinement may be needed at outlier stations to address local variability.

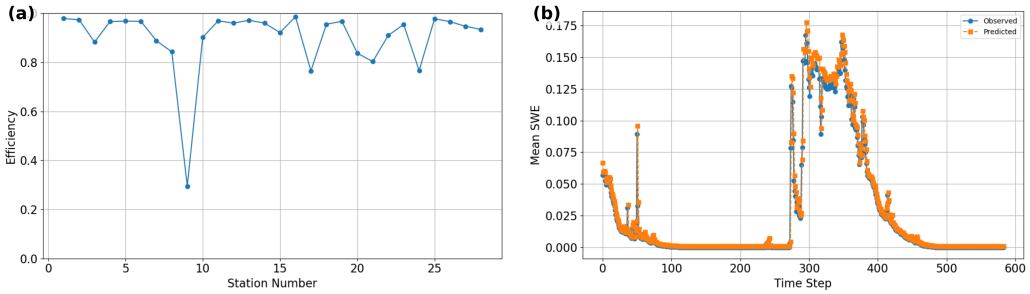

Figure 4: SWE prediction using 1-day data: (a) Efficiency of SWE predictions at 29 stations in New Mexico, (b) Mean SWE values across different time steps.

4.1.2 Prediction Using 2-Day Data

The Snow Water Equivalent (SWE) analysis for New Mexico using two-day prediction data is shown in Figure 5. Panel (a) illustrates the efficiency across stations, where values generally remain high, but compared to the one-day analysis, there is a slightly improved consistency with fewer extreme outliers, suggesting that aggregating over two days helps stabilize prediction accuracy. Panel (b) presents the comparison between observed and predicted SWE, showing that the two-day input captures the seasonal accumulation and melt dynamics with smoother alignment and fewer short-term fluctuations than the one-day results. While small deviations persist around peak accumulation periods, the overall agreement demonstrates that extending the input window to two days enhances the model's robustness in reproducing SWE dynamics and reduces local variability at individual stations.

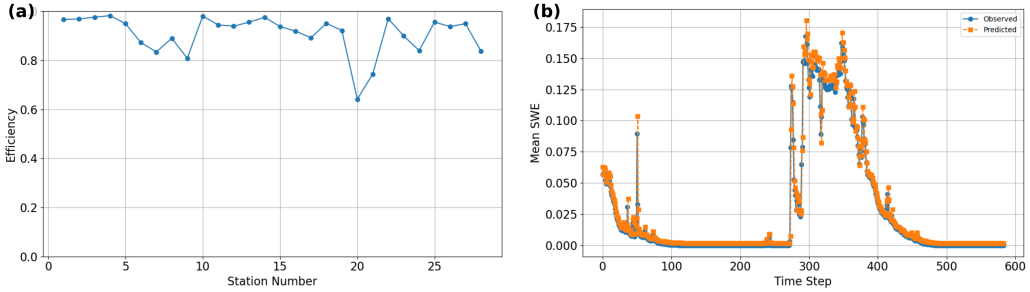

Figure 5: SWE prediction using 2-day data: (a) Efficiency of SWE predictions at 29 stations in New Mexico, (b) Mean SWE values across different time steps.

4.1.3 Prediction Using 3-Day Data

The Snow Water Equivalent (SWE) analysis for New Mexico using three-day prediction data is presented in Figure 6. Panel (a) shows that the station-wise efficiency remains high overall, with most stations above 0.85 and fewer extreme deviations compared to the one-day and two-day results, indicating that the use of three-day input

further stabilizes prediction accuracy across locations. Panel (b) illustrates the comparison between observed and predicted SWE, where the three-day data clearly improves temporal alignment, reducing fluctuations and capturing both accumulation and melt cycles more smoothly. Although slight deviations are still observed during peak snow accumulation periods, the model demonstrates stronger consistency with observed values when extended to a three-day input window. These results suggest that incorporating longer temporal input windows enhances the robustness of SWE predictions, minimizing localized variability and improving regional-scale agreement.

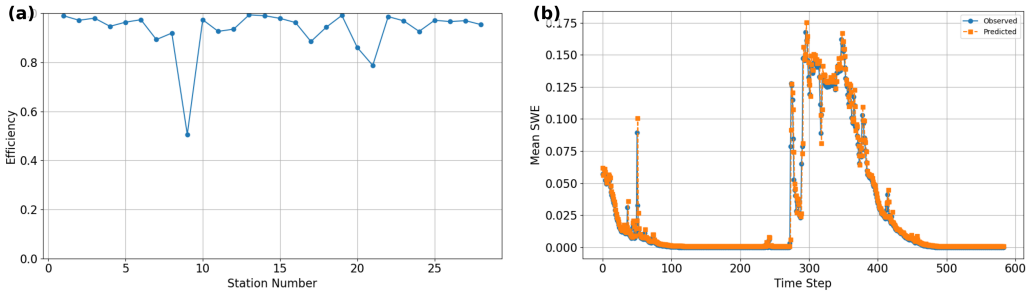

Figure 6: SWE prediction using 2-day data: (a) Efficiency of SWE predictions at 29 stations in New Mexico, (b) Mean SWE values across different time steps.

4.1.4 Prediction Using 4-Day Data

The Snow Water Equivalent (SWE) analysis for New Mexico using four-day prediction data is shown in Figure 7. Panel (a) demonstrates that station-wise efficiency values remain consistently high across most locations, with the majority exceeding 0.85, although a few stations still show noticeable drops, reflecting localized prediction challenges. Compared to shorter input windows, the four-day results show reduced variability between stations, indicating greater stability in predictive performance. Panel (b) illustrates the comparison of observed and predicted SWE, where the four-day input captures both accumulation and melt cycles with smoother alignment and fewer short-term mismatches. While slight deviations remain during peak accumulation periods, the overall temporal match is strong, suggesting that extending the input window to four days improves the robustness of SWE predictions, reduces noise, and enhances agreement at the regional scale.

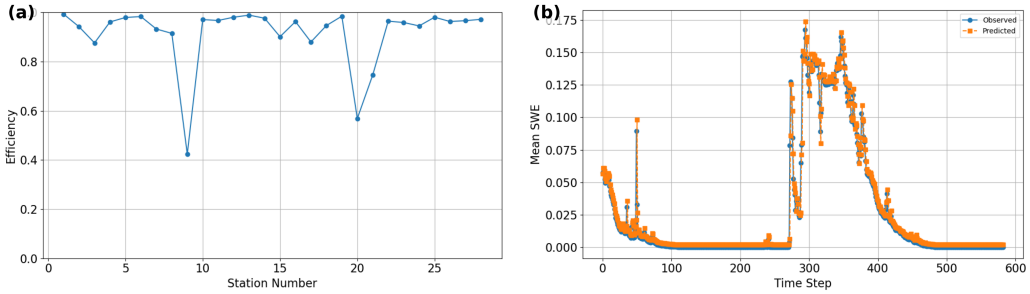

Figure 7: SWE prediction using 2-day data: (a) Efficiency of SWE predictions at 29 stations in New Mexico, (b) Mean SWE values across different time steps.

4.1.5 Prediction Using 5-Day Data

The Snow Water Equivalent (SWE) analysis for New Mexico using five-day prediction data is presented in Figure 8. Panel (a) shows that efficiency across stations remains high, with most values above 0.85, indicating strong predictive skill. However, a few stations still exhibit noticeable drops in efficiency, suggesting localized

prediction challenges that persist even with longer input windows. Compared to the shorter-day results, the five-day input produces more uniform performance across stations, reducing variability. Panel (b) compares observed and predicted SWE time series, showing that the five-day input window captures accumulation and melt cycles with very close agreement, maintaining smooth alignment throughout most of the season. Minor mismatches occur at peak accumulation, but overall the five-day results reflect enhanced temporal stability and regional-scale reliability of the model predictions.

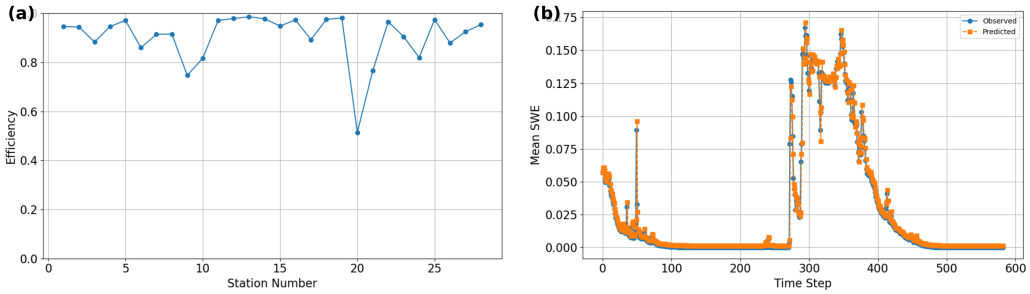

Figure 8: SWE prediction using 2-day data: (a) Efficiency of SWE predictions at 29 stations in New Mexico, (b) Mean SWE values across different time steps.

The spatial prediction results of SWE across New Mexico (Fig. 9) and the tabulated station-wise efficiencies (Table 1) demonstrate that the model maintains strong predictive performance across multiple forecast horizons (1–5 days). Most stations sustain high prediction values in the range of 0.85–0.99, indicating stable model efficiency over space and time. The figure highlights that 1-day and 2-day forecasts exhibit the most consistent performance, while longer forecasts (3–5 days) show only minor spatial variability. The table further confirms this trend, where the majority of stations retain values above 0.90, with only a few locations (e.g., Lat. 36.17716, Lon. -108.94556 and Lat. 33.40682, Lon. -105.79467) showing larger variability or localized decreases in predictive skill. Overall, the combined spatial and temporal analysis demonstrates that the model effectively captures SWE dynamics in New Mexico with high accuracy, and although minor degradation occurs at extended forecast horizons, predictive reliability remains robust even up to 5 days.

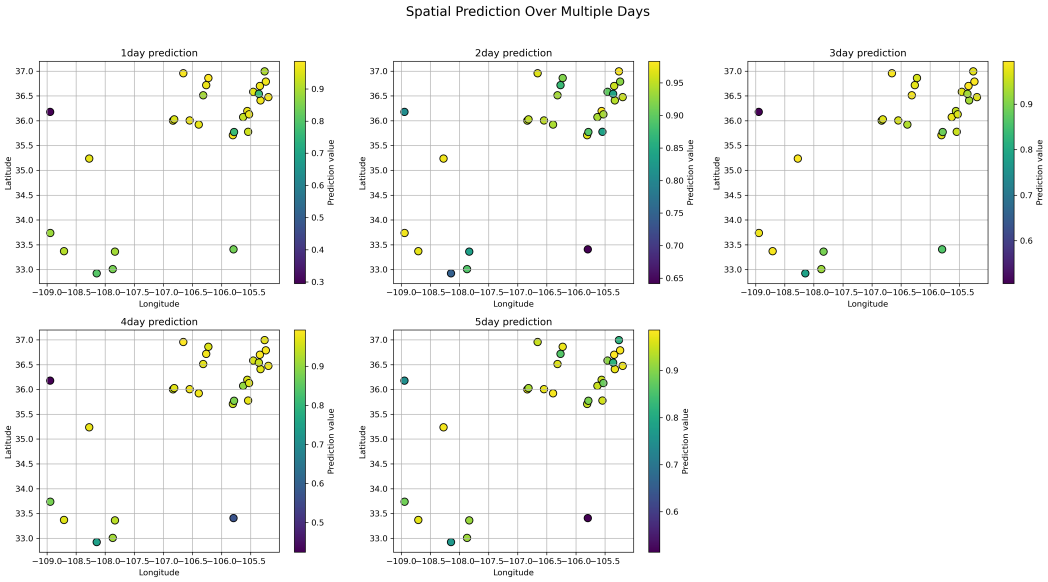

Figure 9: SWE prediction using 2-day data: (a) Efficiency of SWE predictions at 29 stations in New Mexico, (b) Mean SWE values across different time steps.

Table 1: *Station locations and their corresponding efficiency values.*

Latitude	Longitude	1day	2day	3day	4day	5day
36.51174	-106.31543	8.94E-01	9.37E-01	9.88E-01	9.70E-01	9.63E-01
36.95606	-106.65723	9.79E-01	9.67E-01	9.90E-01	9.93E-01	9.46E-01
35.70730	-105.80584	9.74E-01	9.69E-01	9.72E-01	9.42E-01	9.44E-01
33.73687	-108.94327	8.83E-01	9.76E-01	9.81E-01	8.76E-01	8.83E-01
36.19418	-105.55742	9.67E-01	9.83E-01	9.47E-01	9.61E-01	9.46E-01
36.00469	-106.54805	9.68E-01	9.50E-01	9.64E-01	9.80E-01	9.71E-01
36.71632	-106.26370	9.67E-01	8.73E-01	9.74E-01	9.83E-01	8.60E-01
33.36089	-107.83203	8.89E-01	8.34E-01	8.93E-01	9.33E-01	9.14E-01
33.00796	-107.86982	8.43E-01	8.90E-01	9.20E-01	9.15E-01	9.16E-01
36.17716	-108.94556	2.95E-01	8.08E-01	5.06E-01	4.24E-01	7.47E-01
36.99396	-105.25988	9.02E-01	9.81E-01	9.74E-01	9.71E-01	8.17E-01
36.40869	-105.33038	9.70E-01	9.45E-01	9.27E-01	9.67E-01	9.72E-01
35.92195	-106.39179	9.60E-01	9.40E-01	9.36E-01	9.81E-01	9.79E-01
36.69935	-105.34145	9.72E-01	9.56E-01	9.94E-01	9.89E-01	9.86E-01
35.23658	-108.27404	9.60E-01	9.76E-01	9.91E-01	9.77E-01	9.78E-01
36.07196	-105.62949	9.22E-01	9.38E-01	9.80E-01	9.01E-01	9.48E-01
36.85967	-106.22657	9.86E-01	9.19E-01	9.63E-01	9.63E-01	9.73E-01
35.77154	-105.78487	7.65E-01	8.92E-01	8.85E-01	8.80E-01	8.93E-01
36.00152	-106.83408	9.56E-01	9.51E-01	9.44E-01	9.47E-01	9.75E-01
36.78765	-105.23920	9.68E-01	9.22E-01	9.92E-01	9.85E-01	9.82E-01
33.40682	-105.79467	8.38E-01	6.42E-01	8.61E-01	5.69E-01	5.14E-01
32.92342	-108.14546	8.03E-01	7.45E-01	7.88E-01	7.46E-01	7.66E-01
33.36960	-108.70711	9.10E-01	9.70E-01	9.87E-01	9.65E-01	9.66E-01
36.58195	-105.45617	9.55E-01	9.00E-01	9.70E-01	9.59E-01	9.05E-01
36.54099	-105.35944	7.67E-01	8.40E-01	9.26E-01	9.45E-01	8.20E-01
36.47498	-105.19534	9.78E-01	9.56E-01	9.72E-01	9.81E-01	9.74E-01
36.12790	-105.52706	9.66E-01	9.38E-01	9.67E-01	9.63E-01	8.79E-01
36.02653	-106.81361	9.47E-01	9.50E-01	9.70E-01	9.67E-01	9.25E-01
35.77584	-105.54337	9.34E-01	8.38E-01	9.54E-01	9.72E-01	9.54E-01

4.2 Spatial Analysis

To evaluate the spatial accuracy of the ConvLSTM model, raster maps of both observed and predicted Snow Water Equivalent (SWE) were generated. These maps illustrate how closely the model's predictions align with the actual SWE distribution across Northern New Mexico. As shown in Figure 14 the predicted SWE values closely match the observed patterns, particularly in high-elevation areas where snow accumulation is most significant. Minor discrepancies are present in lower-elevation zones, which may be attributed to variability in terrain and data sparsity. Table 1 and Figure 9 demonstrate the model's capability to accurately replicate spatial snow patterns

4.2.1 Prediction Using 1-Day Data

Figure 10 presents the spatial distribution of Snow Water Equivalent (SWE) for one-day input data, comparing observed values (panel a) with model predictions (panel b). The observed map shows SWE concentrated primarily in the northern and northwestern regions, with values exceeding 0.7 in localized zones, while much of the southern and central areas remain snow-free. The predicted map captures this spatial pattern effectively, reproducing the major accumulation zones and their intensities. Minor differences are visible in some smaller patches, where the predicted SWE slightly underestimates or overestimates local magnitudes. Nevertheless, the model successfully replicates the overall spatial extent and gradients of SWE across the domain, demonstrating that a one-day input window is sufficient for resolving large-scale patterns of snow accumulation, though finer local variations remain a challenge.

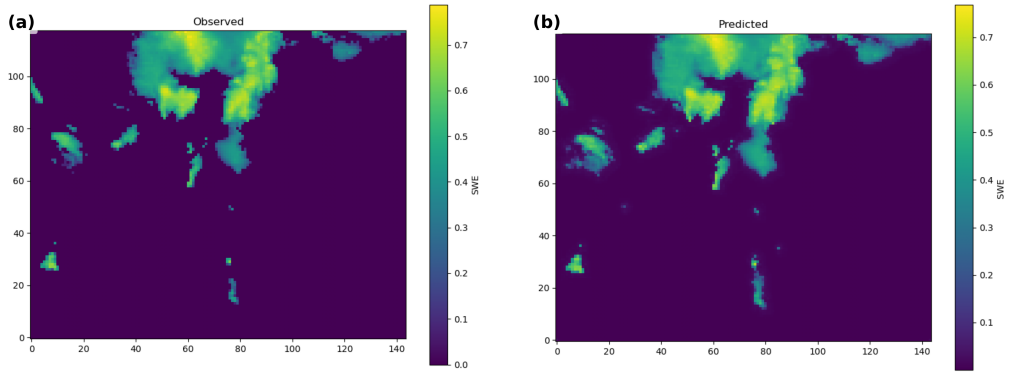

Figure 10: SWE prediction in the study are: (a) Observed , (b) Predicted using 1-day data

4.2.2 Prediction Using 2-Day Data

Figure 11 presents the spatial distribution of Snow Water Equivalent (SWE) for two-day input data, with observed values shown in panel (a) and model predictions in panel (b). The observed map indicates higher SWE concentrations in the northern and northwestern regions, with peak values exceeding 0.7, while central and southern areas remain largely snow-free. The predicted map reproduces these broad spatial patterns effectively, capturing both the extent and magnitude of major accumulation zones. Compared to the one-day results, the two-day input provides smoother agreement between observed and predicted SWE, reducing small-scale discrepancies and noise in patchy regions. Nonetheless, minor mismatches remain in some localized clusters, where the model either underestimates or slightly shifts SWE intensity. Overall, the two-day input enhances spatial stability and improves the replication of large-scale snow accumulation patterns across the study domain.

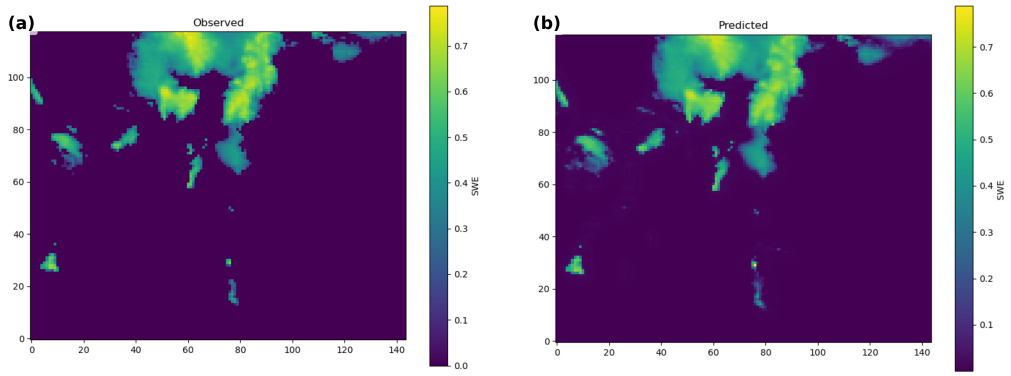

Figure 11: SWE prediction in the study are: (a) Observed , (b) Predicted using 2-day data

4.2.3 Prediction Using 3-Day Data

Figure 12 illustrates the spatial distribution of Snow Water Equivalent (SWE) for three-day input data, with observed SWE shown in panel (a) and predicted SWE in panel (b). The observed map highlights concentrated SWE accumulation in the northern and northwestern portions of the domain, with peak values exceeding 0.7, while the central and southern regions remain largely snow-free. The predicted map successfully reproduces these large-scale spatial patterns, capturing both the extent and intensity of major accumulation areas. Compared to the one-day and two-day results, the three-day input provides improved spatial coherence, with reduced patchiness and a closer match in SWE magnitudes across the accumulation zones. Minor discrepancies remain in some localized patches, where the model slightly underestimates SWE magnitude, but overall the three-day input

demonstrates enhanced ability to replicate observed snow distribution with greater stability and less noise.

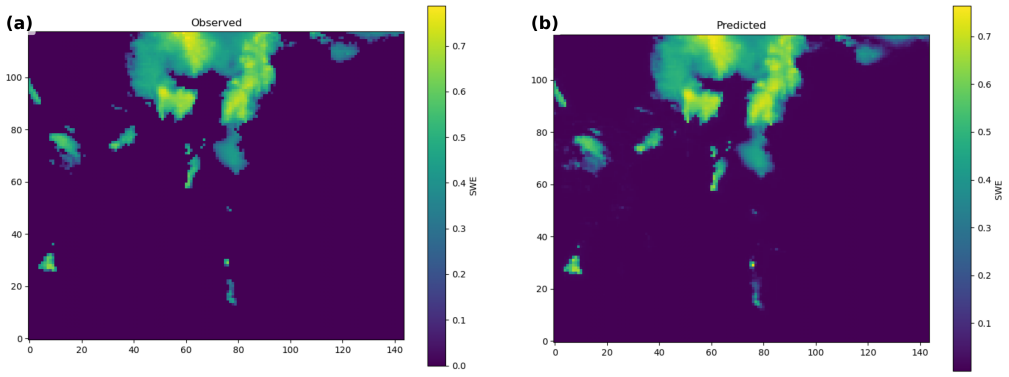

Figure 12: SWE prediction in the study are: (a) Observed , (b) Predicted using 3-day data

4.2.4 Prediction Using 4-Day Data

Figure 13 presents the observed (a) and predicted (b) Snow Water Equivalent (SWE) distributions for four-day input data. The observed map highlights major SWE accumulation in the northern and northwestern regions, with peak values exceeding 0.7, while the southern portions remain largely snow-free. The predicted map reproduces these large-scale accumulation patterns with notable accuracy, particularly in the extent and intensity of the snow-rich northern zone. Compared to the three-day results, the four-day input further improves spatial consistency, reducing localized noise and enhancing the match between observed and predicted SWE fields. Small discrepancies remain in certain scattered patches, where the model slightly underestimates SWE intensity, but overall the four-day configuration demonstrates stronger agreement with observed data, indicating that increased temporal input helps stabilize spatial predictions.

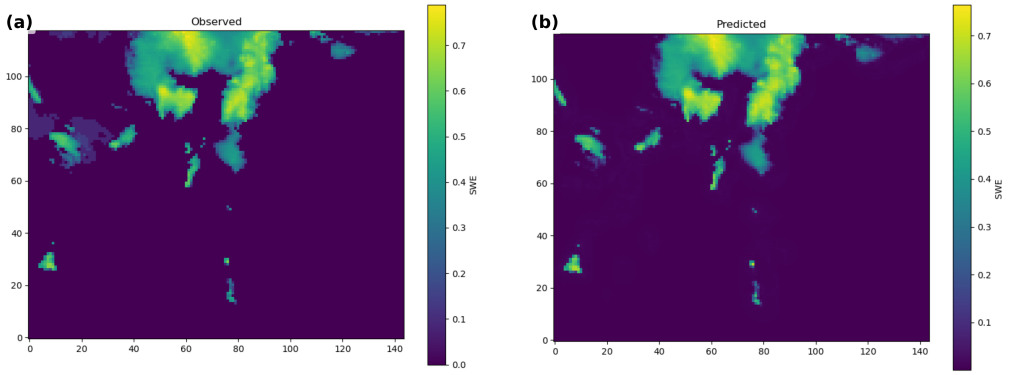

Figure 13: SWE prediction in the study are: (a) Observed , (b) Predicted using 4-day data

4.2.5 Prediction Using 5-Day Data

Figure 14 compares the observed (a) and predicted (b) Snow Water Equivalent (SWE) fields using five-day input data. The observed map shows strong SWE accumulation in the northern region, with peak values exceeding 0.7, and scattered patches in the western and central parts of the domain. The predicted distribution closely replicates the spatial extent and magnitude of these snow-rich regions, indicating that the five-day temporal input improves the model's ability to capture both large-scale and localized SWE variations. Compared to shorter input windows (one- to four-day), the five-day predictions provide a smoother and more stable representation of SWE

while reducing noise in low-accumulation areas. Minor underestimations remain in some scattered zones, yet the overall agreement between observed and predicted maps is strong, confirming that increasing temporal depth enhances the model's spatial generalization and predictive reliability.

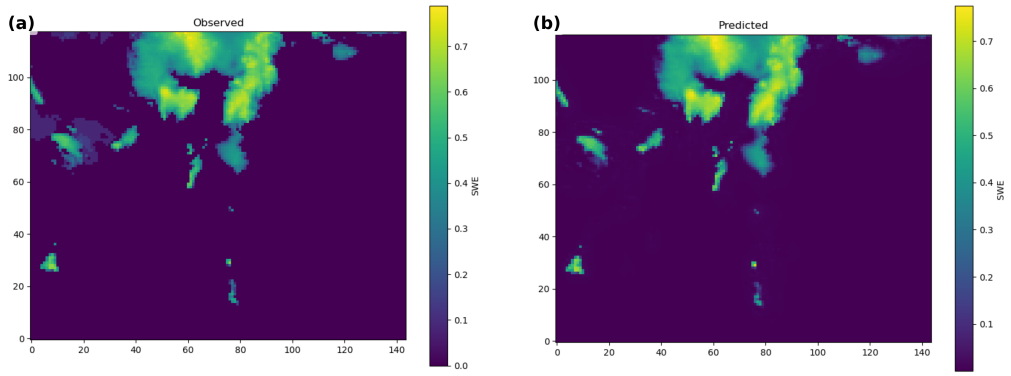

Figure 14: SWE prediction in the study are: (a) Observed , (b) Predicted using 5-day data

5 Discussion

The statistical analyses (Figure 4 – 8) for 1–5 day input data show that the predictive model consistently achieves high efficiency values across most stations, generally above 0.80, though occasional drops are observed at specific stations. The observed versus predicted SWE time series further demonstrate strong alignment, with the model able to capture both the timing and magnitude of SWE fluctuations. As the temporal input window increases from 1 day to 5 days, the predictions become smoother and better aligned with the observed trends, suggesting that longer input sequences improve temporal stability while reducing short-term noise. The improvements are most evident in the later days, where predicted peaks and recessions of SWE closely track observed variations.

The temporal spatial maps (Figure 10–11) provide further evidence of the model's effectiveness in capturing SWE dynamics across the study domain. For short input windows (1–2 days), the model is able to replicate the general spatial structure of SWE, including accumulation in the northern region and smaller scattered patches elsewhere. However, minor underestimations and spatial noise are more pronounced. With 3–5 day input data, the model performance improves noticeably: SWE patterns become smoother, noise in low-accumulation regions is reduced, and high-accumulation zones are captured with greater fidelity. By the 5-day case, the observed and predicted maps show strong similarity in both magnitude and extent, confirming the value of incorporating longer temporal windows for improving spatial generalization.

Although one of the study's objectives was to forecast SWE changes for the next 30 years under different climate scenarios, this could not be fully realized due to weak statistical relationships between SWE and the projected precipitation and temperature data. The ConvLSTM model did not establish significant correlations, indicating that SWE dynamics in northern New Mexico may be influenced by additional factors beyond simple precipitation and temperature inputs, such as snowpack accumulation processes, sublimation, soil moisture, and topographic heterogeneity. Previous studies have also highlighted that in semi-arid and mountainous regions, SWE trends are often decoupled from regional-scale temperature and precipitation signals due to complex snow–climate interactions and local variability. Consequently, while the current model performed well for short-term predictions (1–5 days), long-term projections will require incorporation of downscaled climate data, coupled hydrologic–climate modeling, or enhanced feature engineering to better capture the drivers of SWE variability in the region. This limitation emphasizes the need for further research to bridge the gap between short-term statistical accuracy and long-term climate-informed forecasts.

6 Conclusion

The combined statistical and spatial analyses demonstrate that the predictive model is effective in estimating SWE across both temporal and spatial dimensions. The statistical results highlight consistently high efficiencies and strong agreement between observed and predicted time series, while the spatial maps confirm the model's ability to replicate the geographic distribution of SWE. Importantly, increasing the temporal input from 1 to 5 days improves predictive accuracy, reduces noise, and enhances spatial fidelity. These findings suggest that multi-day temporal integration significantly strengthens the model's robustness, making it more reliable for both point-based predictions and spatially distributed SWE mapping. This approach can therefore serve as a useful tool for snowpack monitoring and water resource management in data-limited regions.

Potential Beneficiaries of the Research

The results of this research will primarily benefit local and regional water managers who rely on snowpack information to guide short-term decision making. By providing insight into the performance of SWE predictions across multiple time horizons, the findings can help irrigation districts, watershed councils, and community-level water boards improve planning for snowmelt-driven water supply. Even though the forecasts are limited in long-term application, the short- to medium-term results can still support local users in adjusting irrigation schedules, monitoring streamflow conditions, and preparing for seasonal variability, ultimately contributing to more informed and adaptive water management at the community scale.

Presentations

- **Snow Water Equivalent Prediction for Northern New Mexico Using the Convolutional LSTM Machine Learning Method** 69th Annual New Mexico Water Conference, hosted by the New Mexico Water Resources Research Institute (NM WRRI), NM, 2024. *Poster Presentation.*
- **Snow Water Equivalent Prediction for Northern New Mexico Using the Convolutional LSTM Machine Learning Method** CIROH (Cooperative Institute for Research to Operations in Hydrology) Annual Conference, University of Vermont, Burlington, VT, 2025. *Poster Presentation.*

Use of Student Grant "NMWRRI-SG-FALL2024."

- New Mexico Water Conference = $394.60
- CIROH Annual Conference, University of Vermont, Burlington, VT, 2024 = $1659.79
- Summer Salary = $5345.61
- Remaining = $100.00

Degree Completion and Future Career Plans

I am currently pursuing a Ph.D. in Civil Engineering with a specialization in Water Resources Engineering at New Mexico State University and am expected to graduate in 2028. My research focuses on snow hydrology, hydrologic modeling, and water resources management, supported in part by the student grant. After completing my degree, I plan to continue working in the field of water resources, with a particular interest in hydrologic modeling, climate resilience, and water management applications. I aim to pursue a career in academia, research

institutions, or applied water agencies where I can contribute to solving critical water challenges in New Mexico and beyond.

Acknowledgment

I gratefully acknowledge the support of the New Mexico Water Resources Research Institute (NM WRRI) Student Water Research Grant, funded by the New Mexico Legislature. This funding provided essential support for my doctoral research in water resources engineering, enabling me to advance my work on snow hydrology and model development. I also extend my sincere appreciation to my faculty advisor and colleagues at New Mexico State University for their guidance and encouragement throughout this project. I would like to sincerely thank Dr. Baokun Li for his foundational work in developing the original code at The Computational Lab for Advanced Water Resources Informatics and Modeling (CLAWRIM). I also thank Mahesh Maddineni for his efforts in modifying and extending the code.

References

- Sturm, M., Taras, B., Liston, G. E., Derksen, C., Jonas, T., & Lea, J. (2010). Estimating Snow Water Equivalent Using Snow Depth Data and Climate Classes. Journal of Hydrometeorology, 11(6), 1380-1394. doi:10.1175/2010JHM1202.1.

- Bartelt, P., & Lehning, M. (2002). A physical SNOWPACK model for the Swiss avalanche warning: Part I. Numerical model. Cold Regions Science and Technology, 35(3), 123-145.

- Niu, G. Y., et al. (2011). The community Noah land surface model with multi-parameterization options (Noah-MP): Model description and evaluation with local-scale measurements. Journal of Geophysical Research: Atmospheres, 116(D12).

- Liang, X., Lettenmaier, D. P., Wood, E. F., & Burges, S. J. (1994). A simple hydrologically based model of land surface water and energy fluxes for general circulation models. Journal of Geophysical Research: Atmospheres, 99(D7), 14415-14428.

- Lawrence, D. M., et al. (2011). Parameterization improvements and functional and structural advances in version 4 of the Community Land Model. Journal of Advances in Modeling Earth Systems, 3(1).

- Chang, A. T. C., Foster, J. L., & Hall, D. K. (1987). Nimbus-7 SMMR derived global snow cover parameters. Annals of Glaciology, 9, 39-44.

- Kelly, R. E. J., Chang, A. T. C., Tsang, L., & Foster, J. L. (2003). A prototype AMSR-E global snow area and snow depth algorithm. IEEE Transactions on Geoscience and Remote Sensing, 41(2), 230-242.

- Rott, H., Nagler, T., & Wiesmann, A. (2010). Snow cover mapping from space using SAR and optical remote sensing. Geoscience and Remote Sensing Symposium (IGARSS), 2010 IEEE International.

- Lievens, H., et al. (2019). Sentinel-1 snow depth retrieval at sub-kilometer resolution over the European Alps. Cryosphere, 13, 1275-1294.

- Painter, T. H., et al. (2016). Airborne snow observatory: Fusion of scanning lidar, imaging spectrometer, and physically-based modeling for mapping snow water equivalent and snow albedo. Remote Sensing of Environment, 184, 139-152.

- Hall, D. K., & Riggs, G. A. (2002). MODIS/Terra Snow Cover 5-Min L2 Swath 500m V005. NASA National Snow and Ice Data Center Distributed Active Archive Center.

- Dozier, J. (1989). Spectral signature of alpine snow cover from the Landsat Thematic Mapper. Remote Sensing of Environment, 28(1), 9-22.

- Margulis, S. A., Girotto, M., Cortés, G., & Durand, M. (2015). A particle batch smoother approach to snow water equivalent estimation. Journal of Hydrometeorology, 16(3), 1752-1772.

- Shi, X., Chen, Z., Wang, H., Yeung, D. Y., Wong, W. K., & Woo, W. C. (2015). Convolutional LSTM Network: A Machine Learning Approach for Precipitation Nowcasting. Advances in Neural Information Processing Systems (NeurIPS), 28, 802-810.

- Wang, H., Xie, L., Luo, H., & Wang, M. (2020). Spatiotemporal Modeling of Snow Water Equivalent Using Convolutional LSTM Networks. Journal of Hydrology, 585, 124801.

- Bi, Y., Fan, K., Xu, J., & Lu, Q. (2020). Improved Snow Depth Prediction Using Convolutional LSTM Networks. Remote Sensing, 12(14), 2285.

- Xingjian, S., Chen, Z., Wang, H., Yeung, D. Y., Wong, W. K., & Woo, W. C. (2015). Convolutional LSTM Network: A Machine Learning Approach for Precipitation Nowcasting. Advances in Neural Information Processing Systems (NeurIPS), 28, 802-810.